Eur. Phys. J. A (2015) **51**: 41
DOI 10.1140/epja/i2015-15041-0

THE EUROPEAN PHYSICAL JOURNAL A

Regular Article – Experimental Physics

Nuclear isomers in ^{259}Sg and ^{255}Rf

S. Antalic[1,a], F.P. Heßberger[2,3], D. Ackermann[2], S. Heinz[2], S. Hofmann[2], B. Kindler[2], J. Khuyagbaatar[2,3], B. Lommel[2], and R. Mann[2]

[1] Department of Nuclear Physics and Biophysics, Comenius University, 84248 Bratislava, Slovakia
[2] GSI-Helmholtzzentrum für Schwerionenforschung GmbH, 64291 Darmstadt, Germany
[3] Helmholtz Institut Mainz, 55099 Mainz, Germany

Received: 22 July 2014 / Revised: 18 February 2015
Published online: 14 April 2015 –
Communicated by R. Krücken

Abstract. The production and radioactive decay of ^{259}Sg and its daughter products were investigated using α-decay spectroscopy and spontaneous-fission measurements. The isotope was produced in the fusion-evaporation reaction ^{206}Pb(^{54}Cr, 1n)^{259}Sg. This work presents first results for isomeric states in the isotopes ^{259}Sg and ^{255}Rf. In addition new results for spontaneous-fission properties and branching ratios of both isotopes are discussed. The new decay-spectroscopy data allowed extending the single-particle systematics of isotones with 151 and 153 neutrons. A change of the ground-state configuration in $N = 153$ isotones from $1/2^+[620]$ to $11/2^-[725]$ was observed for the first time.

1 Introduction

An important issue of theoretical predictions for decay properties of nuclei with unpaired nucleon(s) is the ability to estimate reliably their low-lying single-particle levels. This is an especially critical issue for the region of super-heavy elements where even subtle changes of the level structure could seriously influence their stability and the possibility of their detection. The knowledge of the excited levels and their assignment is very important also for the description of multi-quasiparticle states, that often form K isomers, which are quite frequent in the region of nuclei with $Z \geq 100$ [1]. There are several theoretical models predicting low lying single-particle levels (see, for example, works [2–4]). Any new experimental data for isotopes above fermium ($Z > 100$) serve as very strong test of their quality and are important for their further development.

The experiments aimed at the decay spectroscopy of nuclei in the region of isotopes above fermium ($Z > 100$) are often very difficult due to the low production cross-section which is below one microbarn. However, the development of sensitive experimental techniques for α, γ and also conversion-electron spectroscopy opened the door to study the single-particle level systematics of these nuclei. These techniques brought in recent years significant improvements for single-particle level systematics of einsteinium isotopes ($Z = 99$) [5, 6] and isotones with 147, 149, 151 and 153 neutrons [7–13].

In this paper we present first detailed results for the decay spectroscopy of ^{259}Sg ($Z = 106$) and low-lying levels in its α-decay product ^{255}Rf ($Z = 104$). This work is a continuation of the long-term project at the velocity filter SHIP (Separator of Heavy Ion reaction Products) at GSI Darmstadt aimed at the spectroscopy of transfermium nuclei. In addition we obtained new data for the spontaneous fission (SF) of both isotopes. Besides new spectroscopic data we present in this paper new results for single-particle level systematics of $N = 151$ and 153 isotones.

2 Experiments

We produced the isotope ^{259}Sg in the fusion-evaporation reaction ^{206}Pb(^{54}Cr, 1n)^{259}Sg. The pulsed ^{54}Cr^{8+} beam (5 ms beam-on/15 ms beam-off) was delivered by the UNILAC accelerator with a typical beam intensity of 0.72 pμA (1 pμA $= 6.24 \times 10^{12}$ particles/s). We varied the beam energy from 257 to 270 MeV in order to cover the whole excitation function for the one-neutron evaporation channel and optimized the beam energy for highest possible yield. As target material we used thin foils consisting of the chemical compound ^{206}PbS, with the enrichment above 99.8% for the ^{206}Pb. The targets were produced by evaporation of 450 μg/cm^2 ^{206}PbS material onto 40 μg/cm^2 carbon backings (mounted upstream) and covered by 10 μg/cm^2 carbon to reduce the sputtering of the target material and to increase the target emissivity for better thermal cooling.

[a] e-mail: Stanislav.Antalic@fmph.uniba.sk

Evaporation residues (ERs), recoiling out of the target with a kinetic energy of $\approx 50\,\mathrm{MeV}$, were separated from the primary beam and products from reactions other than complete fusion by the velocity filter SHIP [14]. Separated nuclei were afterwards implanted into a position-sensitive 16-strip silicon detector (PSSD) placed at the focal plane of the separator [15]. The energy resolution of PSSD strips for α particles at $E = 8$–$10\,\mathrm{MeV}$ was typically $\approx 30\,\mathrm{keV}$ (FWHM). The energy thresholds for a low-energy event (α particle, electron, etc.) in the PSSD registered by our data acquisition system was set to 40 keV —slightly above the noise level. The dead time of the acquisition system was $\approx 25\,\mu\mathrm{s}$ after the registration of an event.

For assignment of registered events we used the time and position correlations of signals for implantation of ERs into the PSSD, their radioactive decay and decays of daughter nuclei [16]. Of specific importance for the investigation of isomeric states decaying by internal transitions is the registration of conversion electrons (CE), when indicated also in coincidence with gamma quanta, down to energies of some tens of keV. This method had been proven to be a strong tool already in early experiments at SHIP [17]. It was suggested for investigation of the K-isomers in the heaviest nuclei a couple of years ago [18] and has been successfully applied for several cases since then.

The PSSD was surrounded by six multi-strip detectors (in total combined to 28 strips; denoted as BOX detector in the following text) which were used to detect escaping α particles or fission fragments. Both detectors, BOX together with PSSD, were covering $\approx 80\%$ of the upstream hemisphere.

We used two time-of-flight (TOF) detectors installed in front of the PSSD detector [19]. By (anti)coincidence condition it was used to distinguish signals from radioactive decay and signals from implantation of nuclei. In addition the TOF system allowed us to distinguish projectiles, scattered target nuclei, transfer-reaction products and evaporation residues by measuring their TOF value and the kinetic energy of nuclei implanted into the PSSD. The detector system, together with correlation method, allows the study of products from reactions with low production cross-sections where an extreme sensitivity is required. More details are given elsewhere [20].

A germanium clover detector with four crystals of (50–55) mm diameter and 70 mm length assembled to form a block of $(102 \times 102 \times 70)\ \mathrm{mm}^3$ was placed in close geometry to the PSSD. The calibration of the germanium detector was performed using external γ sources of ^{133}Ba and ^{152}Eu. The efficiency for α-γ coincidences of the PSSD and the germanium clover detector was around (12–15)% for γ transitions with (100–300) keV.

In the final analysis of α-decay spectroscopy data we included also data from an older study in which the fusion-evaporation reaction $^{207}\mathrm{Pb}(^{54}\mathrm{Cr}, 2\mathrm{n})^{259}\mathrm{Sg}$ was used. Part of these results was published already before [21]. The number of events from the reaction with the ^{207}Pb target included in this work was around 10% of the total statistics. However due to the contribution of ^{260}Sg in these data, produced via one neutron evaporation, we did not include the fission events from this reaction to the analysis presented in this paper.

The typical energy losses and implantation depth of ^{259}Sg nuclei were estimated using the SRIM-2013 code [22]. Since SRIM allows to calculate the energy losses only up to uranium, values were estimated by extrapolation of energy losses for isotopes with lower proton number and the same mass. For the expected implantation depth of ERs we obtained $\approx 5.9\,\mu\mathrm{m}$.

Alpha-decay hindrance factors (HF) are defined as ratio of experimental and theoretical partial α-decay half-lives. The theoretical half-lives were calculated according to the formalism given in [23] with a parameter modification given in [24].

3 Alpha decay of ^{259}Sg

Previous α-decay studies of ^{259}Sg performed at SHIP revealed two dominant α-decay lines with decay energies of (9550 ± 10) and (9607 ± 10) keV and a weak α-decay activity with energies spread from 9000 to 9500 keV [21]. These results were confirmed by an independent study done at Lawrence Berkeley National Laboratory (LBNL), in which a group of α decays with (9.593 ± 0.046) MeV and several α decays distributed in the range (9.00–9.47) MeV were observed [25].

The α-decay spectra obtained in our present study are shown in fig. 1(a), (c) and (d). Figure 1(a) displays the spectrum taken in the beam-off periods. In the region from 8 to 10 MeV besides the α decays of ^{259}Sg and its daughter decay products ^{255}Rf and ^{251}No (see possible decay products in fig. 2) also the α-decay line from ^{213}Rn (see the peak at 8089 keV) is present which is produced by a few-nucleon transfer reaction. This spectrum is practically free of any additional background. Requiring a correlation with an ER one can effectively select α decays of ^{259}Sg and its daughter nuclei. The time differences between the implantation signal of the ER and α decays (with an upper limit of 10 s) *vs.* the α-decay energy are shown in fig. 1(b). This spectrum shows that below the correlation time of $\Delta T \approx 3000\,\mathrm{ms}$ ($\log(\Delta T) \approx 3.5$) we observe only very few random correlations. A very good test for random correlations is the α decay of ^{213}Rn. Despite of its short half-life $\approx 19.5\,\mathrm{ms}$ we observed only very few correlations with a correlation time below 100 ms. The reason is different energy-TOF distribution of the transfer reaction products and ERs (as an example see fig. 4 in ref. [20]). Most of the correlations for 8089 keV α-decay line are observed with a correlation time above $\approx 3000\,\mathrm{ms}$ ($\log(\Delta T) \geq 3.5$) and represent random correlations. For the α decays of ^{259}Sg we can see a gap between the random correlations and real decays ($\log(\Delta T) < 3.3$–3.4). Therefore for further analysis of ^{259}Sg α decay we limited the correlation time to $\Delta T < 2000\,\mathrm{ms}$ ($\log(\Delta T) < 3.3$).

Our new results confirm the existence of both main α-decay lines with energies of (9550 ± 8) and (9614 ± 8) keV reported in previous studies. As is already indicated in the two-dimensional plot in fig. 1(b), there is a slight

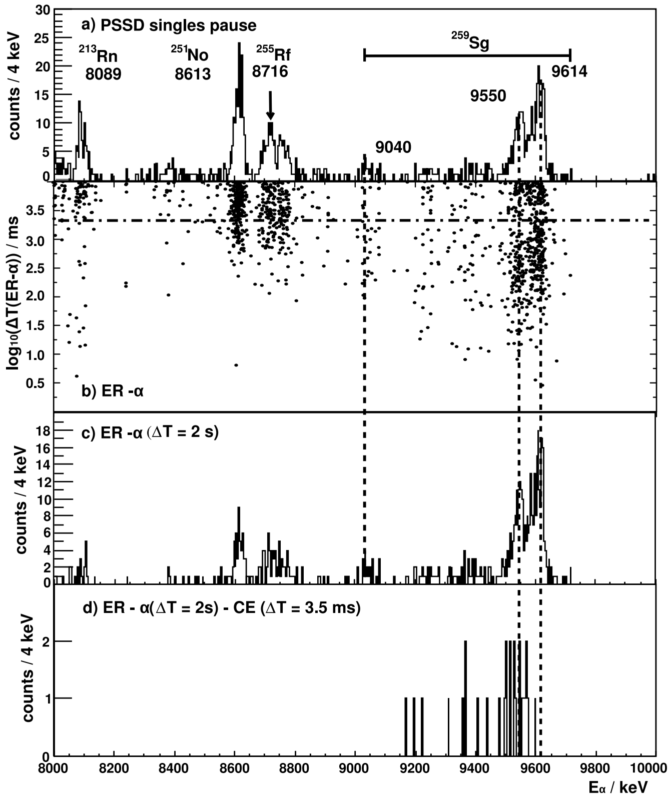

Fig. 1. Spectra of α decays obtained in the production of ^{259}Sg. Panel (a) shows the α-decay spectrum measured in the beam pause. Panel (b) shows the 2D spectrum of correlation time in logarithmic scale *vs.* the α-decay energy for all α decays in the beam pause following an ER implantation signal within 10 s correlation time and 0.6 mm position window. The dot-dashed line at $\log(\Delta T) \approx 3.3$ represents the limit for real correlations. Panel (c) shows part of these α decays with the correlation time up to the 2 s. Panel (d) shows α decays from panel (c) followed by an electron signal within 3.5 ms in the same strip. Energy values are given in keV.

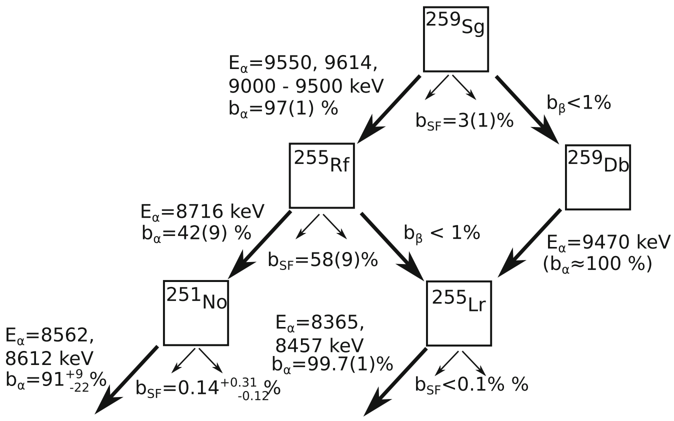

Fig. 2. Sketch of the possible decay modes for ^{259}Sg and its daughter products. Values for ^{259}Sg and the limit for EC/β^+ decay of ^{259}Db are from this work. Some values for ^{255}Rf and ^{251}No are from [26]. All other values are from NNDC [27].

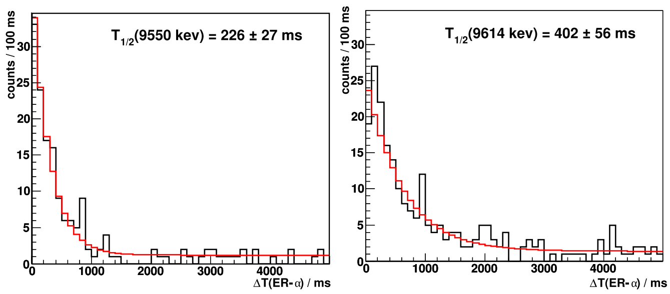

Fig. 3. Decay curves for two strongest α transitions with energies 9550 keV (left panel) and 9614 keV (right panel). Red function represents the fit by exponential function combined with constant background.

difference in the time distributions ΔT(ER-α) for both lines. From the fit of time distributions for ER-α correlations registered within 2 s correlation time we evaluated for the 9550 keV line a half-life of (226 ± 27) ms and for the 9614 keV transition (402 ± 56) ms (see fig. 3). As the alpha lines are not fully separated there might be in each time distribution shown in fig. 3 a small contribution ($< 5\%$) from the other line. In addition we observed a weak α-decay line at (9040 ± 10) keV (see fig. 1(a)).

Figure 1(d) finally shows the energy distribution of α decays following an ER within two seconds and followed by an electron (low energy signal) within 3.5 ms. Only events between $\approx$ 9150 and 9500 keV are seen, but no events within the line at 9040 keV and around the maximum of the one at 9615 keV. The broad distribution of events in the range from 9150 to 9500 keV is interpreted as due to the energy summing of conversion electrons and α particles. The concentration around 9200 keV is interpreted as due summing of alpha particles and electrons leaving the detector almost perpendicular to the detector surface. This leads to minimum energy loss and consequently to minimum energy summing.

The evaluated half-lives for the two strongest lines indicate the existence of two long-lived states. Since the full-energy events distributed from 9000 to 9100 keV exhibit a half-life 440^{+91}_{-64} ms we assigned the 9040 keV line as α decay from the state with (402 ± 56) ms half-life with relative intensity of $\approx 11\%$. On the other hand the half-life of events distributed from 9200 to 9400 keV is 280^{+40}_{-31} ms. Therefore we assigned these events as α decays from the same state as the strong 9550 keV line. Finally, we observed nine ER-α correlations with α-decay energies from 9690 to 9730 keV fully stopped in the PSSD with a half-life of 260^{+142}_{-68} ms. Despite of the large uncertainty it is more likely that these α decays represent a transition from the same level as 9550 keV decays.

Figure 4 shows all α-α correlations within a position window of 0.6 mm and a correlation time limit of 30 s. We marked by rectangles five main groups of correlations.

Region A covers the correlations of ^{259}Sg with the decay of its α-decay daughter product ^{255}Rf. Regions B and C cover correlations of ^{255}Rf and ^{259}Sg with their α-decay product — ^{251}No. The daughter energy obtained for both groups of (8614 ± 14) keV agrees well with the known α-decay energy of ^{251g}No of (8612 ± 4) keV. The

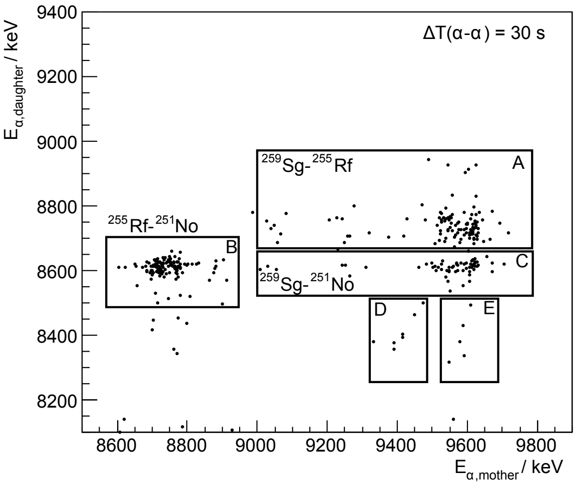

Fig. 4. Spectrum for α-α correlations for the experiment with main part of ^{259}Sg data. The position window was chosen 0.6 mm and the correlation time window 30 seconds. One α decay from the correlation pair was required to be in the beam-pause period.

non-observation of correlations for α decays of ^{255}Rf and from the long-lived isomeric state in ^{251}No with half-life of (1.02 ± 0.03) s is in agreement with the previous study of ^{255}Rf [26].

We further observed a group of 11 α-α correlation events in the energy range $E_{\mathrm{mother}} = (9300–9670)$ keV and $E_{\mathrm{daughter}} = (8290–8485)$ keV (see boxes D and E in fig. 4). Despite a rather long correlation time ($\Delta T(\alpha$-$\alpha) = 30$ s), we did not observe any random correlations for α decays from strongest α lines, *e.g.* correlations with α decays of ^{251}No as mother events with α decays of ^{255}Rf as daughter events. Following the procedure described in [28] we evaluated the probability for a random correlation of two α decays with an energy from 8300 to 9800 MeV to be less than 1%. Therefore we consider all events in the boxes D and E as real α-α correlations.

Possible sources for events in box D in fig. 4, are α-α correlations of ^{259}Db ($E_{^{259}\mathrm{Db}} \approx 9474$ keV [29]) with ^{255}Lr decay ($E_{^{255g}\mathrm{Lr}} \approx 8373$ keV and $E_{^{255m}\mathrm{Lr}} \approx 8467$ keV [6,30]). Events in box E are assigned as α-decay correlations of ^{259}Sg with ^{255}Lr and will be discussed in sect. 6.

There were two production possibilities for ^{259}Db in our experiment. The first is β decay of ^{259}Sg which was not reported until now. The second is the production of ^{259}Db via one proton evaporation channel of the compound nucleus, which should be at least two orders of magnitude weaker compared to the one neutron evaporation channel.

The isotope ^{259}Db was observed in the Heavy Ion Research Facility in Lanzhou (HIRFL) [29]. This isotope is reported to decay by a dominant α transition with an energy of ≈ 9474 keV and its decay pattern overlaps with α decays of ^{259}Sg. However α-α correlation search used in our study allows to distinguish α-decay events of both isotopes (see box D in fig. 4).

Considering the number of events in box D in fig. 4, we estimate for the beta branch in ^{259}Sg an upper limit of 0.01. The relative intensities and hindrance factors for the discussed α transitions of ^{259}Sg are given in table 1.

4 Isomeric state in ^{255}Rf

Besides the ER implantation, spontaneous fission and α decays, the detector system allowed us to measure also the signals from low-energy electrons down to several 10 keV. This is especially important for the detection of long-lived isomeric states, when the de-excitation path goes via one or more converted transitions.

In order to identify a possible isomeric state in ^{255}Rf we applied triple correlation search with chains consisting of ER implantation, α decay and the signal of electrons from internal conversion process (ER-α-CE). The maximum accepted time differences between the ER and α-decay signals were set up to 2 seconds. The time difference for delayed coincidences between the α decay and CE signal was requested up to 3.5 ms. As proper α decays we accepted only events with an energy from 8 to 10 MeV registered by the PSSD or combination of PSSD+BOX detector. In total we observed 42 ER-α-CE chains. Twenty-nine of them were registered with full α-decay energy in the PSSD (see fig. 1(d)). The energy distribution of these α-decay events covers mainly the range of the 9550 keV line and several of them also the energy interval from 9150 to 9550 keV. Therefore we assigned registered electrons to the internal conversion of an isomeric state in ^{255}Rf populated by the α decay of the 226 ms state ^{259}Sg.

The average energy of the registered CEs was $\approx$ 105 keV (see fig. 5). The broad energy distribution is due to a limited energy resolution of the detector strips at such low energies and the uncertainty of the energy calibration which might be for individual strips up to the 10 keV. This arises from the fact, that the PSSD was calibrated using the α-decay energies from reaction products with typical energies of ≈ 7 MeV. From measured time differences between the α decay and CE signal (see the inset in fig. 5) we evaluated a half-life of $(50 \pm 17)\,\mu$s.

Observation of CEs indicates that the excitation energy is by ≈ 105 keV either above the binding energy of the atomic electrons in rutherfordium at K shell with $E_b =$ 156.9 keV or L-binding energy with $E_b = (23–31)$ keV. We did not observe any gamma or X-rays in coincidence with observed CEs. Considering a detection efficiency of 15% in case of emission of K_α or K_β X-rays we would expect six α-X-ray coincidences. The absence of K-X-rays indicates that the isomer predominantly deexcites by internal conversion on the L shell meaning that the transition has either magnetic character with an energy below the K binding energy of rutherfordium or is an electric one. As $E1$ and $E2$ transitions would not lead to isomeric states of some tens of microseconds half-life and for $E3$ or higher multiplicity half-lives considerably higher than a millisecond are expected, we consider the possibility of an electric transition as unlikely. On the other hand, isomeric $5/2^+[622]$ states decaying by $M2$ transition (with $E3$ admixture) into the $9/2^-[734]$ ground states are known in

Table 1. Summary of α-decay transitions for the ground-state decay ^{259g}Sg and decay from the isomeric state ^{259m}Sg. The value $i_{\alpha,rel}$ indicates the relative intensity of the α transition for each long-lived state and $T_{1/2}$ its half-life from experimental data. The column "transition" indicates the initial and final Nilsson level connected by the α-decay transition (see discussion for more details).

E_α/keV	$i_{\alpha,rel}$	$T_{1/2}$/ms	HF	Transition
		^{259g}Sg		
9040 ± 10	0.11 ± 0.02	440^{+91}_{-64}	≈ 5	$11/2^-[725] \rightarrow 11/2^-[725]$
9614 ± 8	0.89 ± 0.02	402 ± 56	≈ 30	$11/2^-[725] \rightarrow 9/2^-[734]$
		^{259m}Sg		
$9200 \pm 25^{(a)}$	0.43 ± 0.04	280^{+40}_{-31}	≈ 2	$1/2^+[620] \rightarrow 1/2^+[620]$
9550 ± 8	0.54 ± 0.04	226 ± 27	≈ 18	$1/2^+[620] \rightarrow 5/2^+[622]$
9700 ± 20	0.03 ± 0.01	260^{+142}_{-68}	≈ 960	$1/2^+[620] \rightarrow 9/2^-[734]$

(a) Line is only tentative.

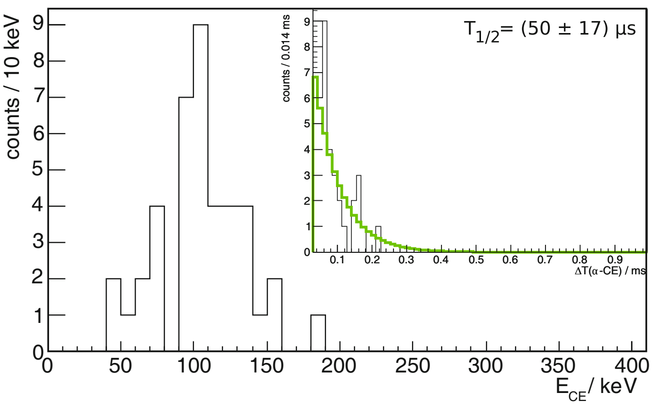

Fig. 5. Spectrum of the conversion electrons measured within 3.5 ms after the α decay of ^{259}Sg. The inset shows the time differences between the α decay and signal from the conversion electrons. Only the first 1 ms is shown, however we did not observe any events with $\Delta T(\alpha\text{-CE})$ difference from 1 ms and 3.5 ms (upper limit of the correlation search).

the lighter $N = 151$ isotones at typical excitation energies from 140 to 250 keV with a lifetime of some tens of microseconds. Considering a binding energy of ≈ 30 keV for rutherfordium L electrons, we can localize the isomer at $E_{exc} \approx 135$ keV, which is, however, regarded as an approximate value due to our limited accuracy of CE energy measurement.

5 Spontaneous fission of ^{259}Sg and ^{255}Rf

The isotope ^{259}Sg may decay by α emission, β decay and spontaneous fission. A spontaneous-fission branch for ^{259}Sg has been reported already from measurements performed at GARIS (Gas-filled Recoil Ion Separator) in RIKEN [31] and at Berkeley Gas-filled Separator in LBNL [32], however in each measurement only one spontaneous fission of ^{259}Sg event was detected. Considering the total statistics from both previous studies one obtains a branching value for spontaneous fission of $0.12^{+0.15}_{-0.08}$.

We registered 393 α decays with the full energy released in the PSSD attributed to ^{259}Sg and 347 spontaneous-fission events in pause between the beam pulses. Most of the fission events have origin in spontaneous fission of ^{255}Rf which has $b_{SF} = 0.52 \pm 0.06$ [33]. The spontaneous fission of two different isotopes (in our case mainly ^{259}Sg and ^{255}Rf) cannot be distinguished and assigned with our experimental set-up only on the basis of the measured energy. However, we used the correlation search with signal from ER implantation and possible α decay to determine the most probable origin of fission events. Generally, a spontaneous-fission event of ^{255}Rf has to be preceded by an α decay of ^{259}Sg and the spontaneous fission of ^{259}Sg and ^{255}Rf was distinguished on the basis of correlations ER-SF(^{259}Sg) or ER-α-SF(^{255}Rf). Following this concept as spontaneous-fission events of ^{259}Sg we considered ER-SF correlations without any full energy or escaped α-decay signal between signals from ER implantation and spontaneous fission within a position window of ± 2 mm. We have to note here, that there is a possibility that an α particle is not correlated to the ER, *e.g.* due to the missing position signals for some of the escaping α particles. We evaluated this probability to be up to the 5% from the number of missing α decays in the triple correlation chains of $\alpha(^{259}\text{Sg})$-$\alpha(^{255}\text{Rf})$-$\alpha(^{251}\text{No})$.

Since the correlation search provide us good selectivity for high-energy events we included in further analysis also events from beam-on period in anti-coincidence with TOF system. From all fission events we attributed 34 events as candidates for spontaneous fission of ^{259}Sg. The time differences from preceding signal (*i.e.* α decay or ER) for spontaneous fission of candidates for ^{259}Sg and ^{255}Rf are shown in fig. 6. Despite of different time distributions, there is still significant overlap. This is critical because of the possibility to consider as a candidates for SF of ^{259}Sg spontaneous-fission events of ^{255}Rf due to the missing link with α particle.

From the time distribution of $\Delta T(\alpha\text{-SF})$ of the ER-α-SF correlations with an α-decay energy in range from 8.95 to 9.75 MeV we obtained a half-life of (1.54 ± 0.19) s for the SF activity, which is in good agreement with the half-life of (1.68 ± 0.09) s reported for ^{255}Rf [26].

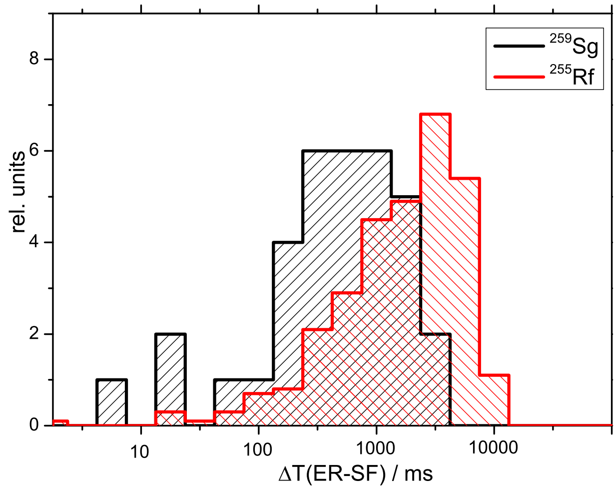

Fig. 6. The distributions for correlations times of events assigned as candidates for spontaneous fission of ^{259}Sg and ^{255}Rf (see the text for more details). The distribution for ^{255}Rf was scaled down by factor of 10 to normalized it on the statistics for ^{259}Sg.

From the time differences of ER-SF correlations attributed to SF activity of ^{259}Sg we evaluated a half-life of 299 ± 147 ms. Taking into the account a back-ground from longer-lived ^{255}Rf activity (see above), which somehow lengthens the half-life value, but is hard to correct due to the quite low number of events, this value suggests a tentative assignment of the fission activity to the decay of the same nuclear level as the short-lived α-decay activity (see sect. 3).

To reduce a possible admixture of ^{255}Rf in the ^{259}Sg dataset we considered in the further analysis only correlations observed with a correlation time up to ΔT(ER-SF) < 950 ms. Within this time we observed 26 candidates for spontaneous-fission events of ^{259}Sg, four of them with the coincidence signal of PSSD and BOX detectors. From number of ER-α-SF with the correlation time of $\Delta T(\alpha\text{-SF}) < 950$ ms we expect that the dataset of ^{259}Sg SF events still contains ≈ 7 events with an origin as spontaneous fission of ^{255}Rf. Considering the 75% duty factor for α decays in pause and $\approx 55\%$ detection efficiency for α decays with full energy release in PSSD and fact that 950 ms interval covers only part of the decay curve the resulting SF branching value of ^{259}Sg is 0.03 ± 0.01.

The fission spectra are shown in fig. 7. Although there is a possibility that both fission fragments are stopped in PSSD, there is also $\approx$ (35–40)% possibility that one fission fragment may escape from the PSSD and might be detected by one of the BOX detectors.. This escape is caused by the significantly lower implantation depth of ERs compared to the range of the fission fragments (typically up to $\approx$ (20–25) μm). Therefore for the TKE evaluation we consider only fission events with a coincident signal from BOX detector and PSSD with both fission fragments registered. The mean energy of four observed events of ^{259}Sg is $E_{mean} = (185 \pm 11)$ MeV with a standard deviation for the fission energy distribution of $\sigma = 20$ MeV. For ^{255}Rf

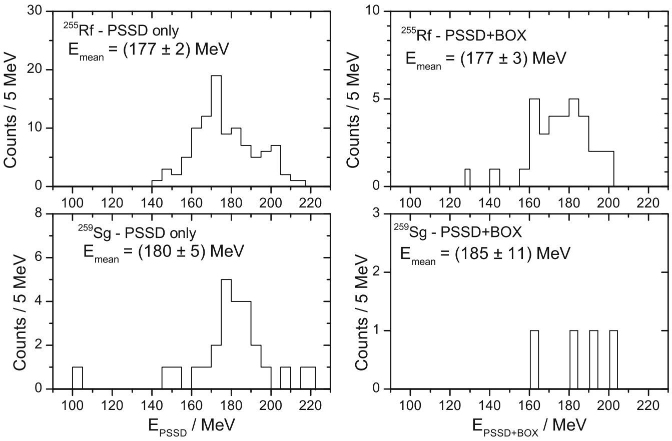

Fig. 7. Comparison of the fission spectra for ^{255}Rf and ^{259}Sg. The upper panels show spectra for ^{255}Rf, the lower panels for ^{259}Sg. On the left are spectra for fission fragment signals registered in the PSSD, on the right are summed signals from PSSD and BOX detector for coincidence events. All events were correlated to the implantation of an ER. Given values for uncertainties are statistical. The energy indicated in the panels is without the correction for the pulse height defect (see the sect. 5 for more details). We note, here, that the signals for escaping fission fragments registered by the BOX detector were quite low (typically only several MeV) which is, together with low statistics, the reason for similar mean energy values of events with signal only from PSSD and for events with coinciding signal from PSSD and BOX detector.

we obtained the value of $E_{mean} = (177 \pm 3)$ MeV with a standard deviation of $\sigma = 16$ MeV. The systematic uncertainty for the energy measurement due to the calibration was evaluated to be ≈ 3 MeV.

The estimated TKE values are influenced by the pulse height defect (PHD), which causes a non-linear detector response for heavy ions. The PHD strongly depends on the atomic number and mass of the considered nucleus. To correct the effect of PHD we applied the method used for estimation of TKE in our previous SHIP experiments where the dependence of the PHD from the implantation depth of fissioning nuclei was investigated [20,34].

Considering the calculated implantation depth of 5.9 μm we obtained the TKE for ^{255}Rf as $E_{TKE,^{255}\text{Rf}} = (199 \pm 3)$ MeV and for ^{259}Sg as $E_{TKE,^{259}\text{Sg}} = (209 \pm 11)$ MeV. For these values we consider an additional systematic uncertainty around ± 10 MeV.

Despite of the large uncertainty, our data for PSSD + BOX coincidences (see fig. 7, right panels) indicate higher TKE for the spontaneous-fission fragments of ^{259}Sg than for ^{255}Rf. The increasing value for the TKE is in agreement with increasing fissility of the nucleus known as Viola-Seaborg systematics [35].

6 Branching ratios of ^{255}Rf

We mentioned in section 3 an indication for α-α correlations of ^{259}Sg and ^{255}Lr (see events at $E_{mother} \approx 9580$ keV —box E in fig. 4).

The beta decay of ^{255}Rf is expected to populate mainly the $7/2^-[514]$ state in ^{255}Lr, since the spin and parity of the ground state in ^{255}Rf was assigned to $9/2^-[734]$ [26]. A direct β decay to the $1/2^-[521]$ state is a fourfold-forbidden transition, however, this state might be populated by an internal transition from the higher-lying $7/2^-[514]$ isomer. One has to note that some α-α correlations in this group may arise from α particles of higher energies from ^{251}No, ^{255}Rf and ^{259}Sg due to α particles escaping the PSSD under small angle with a detector surface and leaving most of their energy in the PSSD. Therefore we consider the number of the events at ≈ 9580 keV in box E in fig. 4 as an upper limit of the ^{259}Sg-^{255}Lr correlations resulting in an upper limit of $b_{EC/\beta^+} < 0.06$ for ^{255}Rf.

For α decay and the spontaneous-fission events (assigned according to procedure described in sect. 5) of ^{255}Rf we obtained the value of $b_{SF} = 0.45 \pm 0.03$ and $b_\alpha = 0.48 \pm 0.03$. These values are in agreement with two recent published values from previous experiments performed at SHIP —$b_{SF} = 0.45 \pm 0.06$ [36] and $b_{SF} = 0.52 \pm 0.06$ [33].

7 Discussion

7.1 Decay of ^{259}Sg and excited states in ^{255}Rf

In table 1 the α-decay lines assigned to the decay of ^{259}Sg are listed. As discussed in sect. 3 we suggest the existence of two long-lived states in ^{259}Sg. The first state with a half-life of (402 ± 56) ms decays by a strong α transition with an energy of (9614 ± 8) keV and a weaker α line of (9040 ± 10) keV. The second state with a (226 ± 27) ms half-life decays mainly by a strong (9550 ± 8) keV α decay and two weaker transitions with energies of (9200 ± 20) keV and (9700 ± 20) keV.

Similar to the α decay of the neighbouring isotone ^{257}Rf [13], the decay pattern observed in the study of ^{259}Sg and the existence of the isomeric state in this isotope, can be explained by the presence of $1/2^+[620]$ and $11/2^-[725]$ Nilsson states with small difference of their energies.

The α-decay spectrum in fig. 1(d) indicates, that the isomeric state in ^{255}Rf is dominantly populated by the α transition with 9550 keV, but not by the 9614 keV transition. Considering the supposed $M2$ character for the internal transition de-exciting the isomeric state to the $9/2^-[734]$ ground state in ^{255}Rf (see discussion in sect. 4) we assign the final state for this α-decay transition as $5/2^+[622]$, which is isomeric having a half-life of $\approx 50\,\mu$s and an excitation energy of ≈ 135 keV. The $5/2^+[622]$ state is also known as an isomeric one in several lighter $N = 151$ isotones with half-lives of several tens of microseconds and the $E_{exc} \approx (140–250)$ keV (see later sect. 7.3).

The α transition with 9550 keV has a low hindrance factor of ≈ 18 and should connect two states with a moderate difference of spin and the same parity. We assign therefore the initial state in ^{259}Sg for this α transition as the $1/2^+[620]$ state. As is discussed in sect. 3 the weak 9700 keV line is assigned to the decay from the same state as well. Due to the high hindrance factor ($HF \approx 960$) we suggest that it populates a state with significantly different spin and opposite parity compared to the initial state (*i.e.* $1/2^+[620]$). Considering also the fact that this is the highest-energy α-decay transition the best candidate for its final state is the ground state of ^{255}Rf assigned as $9/2^-[734]$. The assignment for both lines is supported by the agreement of total Q_α values for the 9550 keV decay populating the level at $E_{exc} \approx 135$ keV and the 9700 keV populating the ground state ($\Delta Q \approx 150$ keV). In addition we assign the tentative α decay with 9200 keV with an estimated $HF \approx 2$ as a transition connecting the $1/2^+[620]$ state in both isotopes —^{259}Sg and ^{255}Rf. The final state should be located roughly at the excitation energy of 510 keV.

Having assigned the 9550 keV transition as a decay from the $1/2^+[620]$ state, the strong 9614 keV transition with $HF \approx 30$ must represent a decay from the $11/2^-[725]$ state in ^{259}Sg either to the $9/2^-[734]$ ground state in ^{255}Rf or to the $11/2^-$ state —first level of the rotational band build upon the ground state of ^{255}Rf. The energy of α particles populating the first excited state of the rotational band is with high probability summed with conversion electrons emitted from the fast low energy $M1$ transition to the $9/2^-[734]$ ground state. Therefore, signals for transition to the $11/2^-$ state are shifted close to the energy for the transitions directly to the $9/2^-[734]$ ground state. Similarly, due to its half-life, the α transition with 9040 keV is assigned as α decay from the same state (see discussion in sect. 3). Due to its low hindrance factor it is interpreted to populate a state with similar spin and the same parity. However, except of the $9/2^-[734]$ ground state, all low-energy states have low spins and positive parities. Therefore we suggest that the 9040 keV transition populates the $11/2^-[725]$ Nilsson level expected from the theoretical predictions at $\approx 850–890$ keV [2, 4]. Considering the Q_α values for the 9614 and 9040 keV decays we suggest that the latter one populates an excited level at ≈ 600 keV. This idea is tentatively supported by the observation of two α events with an energy of ≈ 9040 keV in coincidence with γ cascades of total energy of 594 and 536 keV, respectively. We note, that a similar α-γ coincidence was observed for one event also in the previous studies ($E_\alpha \approx 9050$ keV; $E_\gamma = 593$ keV) [21].

Crucial for the data interpretation was the observation of the isomeric state in ^{255}Rf. As we mentioned, the α-decay energy from the $11/2^-[725]$ Nilsson state to the $9/2^-[734]$ ground state in ^{255}Rf (9614 keV) has a lower value than the transition from the $1/2^+[620]$ level with the highest energy interpreted as decay into the ground state of ^{255}Rf. In addition it has lower energy than the energy sum of the transition into the isomeric $5/2^+[622]$ state (9550 keV) and the excitation energy of this state ($E_{exc} \approx 135$ keV). Therefore the $1/2^+[620]$ state must be located above the $11/2^-[725]$ state. Consequently we assign the ground state in ^{259}Sg as $11/2^-[725]$ and the long-lived excited isomeric state as $1/2^+[620]$. From the difference of Q_α values of 9614 and 9700 keV lines we evaluated the excitation energy of ≈ 90 keV for the isomeric state in ^{259}Sg.

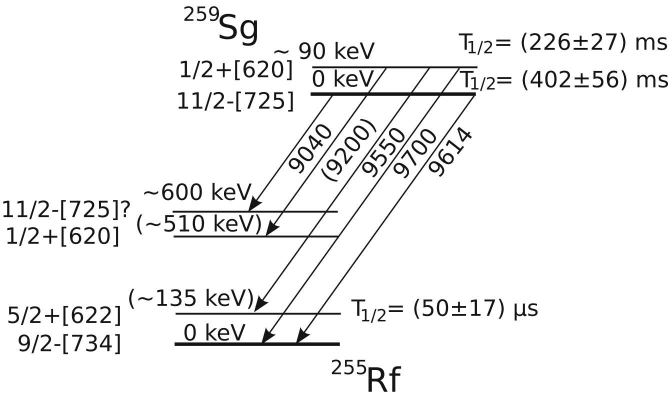

Fig. 8. Suggested decay scheme for α decay of ^{259}Sg from this study (see the text for more details). Values in brackets are tentative.

Considering all discussed single-particle levels, α-decay energies and hindrance factors (see table 1) we suggest for ^{259}Sg the α-decay scheme as shown in fig. 8.

7.2 Hindrance factors for spontaneous fission of ^{255}Rf and ^{259}Sg

A well-known feature of spontaneous fission is the hindrance of the fission processes for nuclei with odd proton and/or odd neutron numbers compared to neighbouring even-even nuclei. Qualitatively this can be explained by spin and parity conservation of the unpaired nucleon, which usually has to keep its level at crossing points of Nilsson levels, while pairs of nucleons may change. Therefore the most favourable fission path may be forbidden, leading to an effective increase of the fission barrier, denoted in the literature as "specialization energy" [37]. Quantitatively this effect can be expressed by a hindrance factor defined as $HF = T_{sf}(Z,N)/T_{ee}(Z,N)$ where $T_{sf}(Z,N)$ is the partial fission half-life and $T_{ee}(Z,N)$ is the unhindered fission half-life obtained as the geometric mean of the fission half-lives of the neighbouring even-even nuclei [38] $T_{ee}(Z,N) = (T_{sf}(N-1,Z) \times T_{sf}(N+1,Z))^{1/2}$ In the case of ^{259}Sg fission half-lives of the neighbouring even-even nuclei are experimentally known, so "pure" experimental hindrance factors can be calculated. We obtained $HF = 8150$ for ^{255}Rf and $HF = 1050$ for ^{259}Sg.

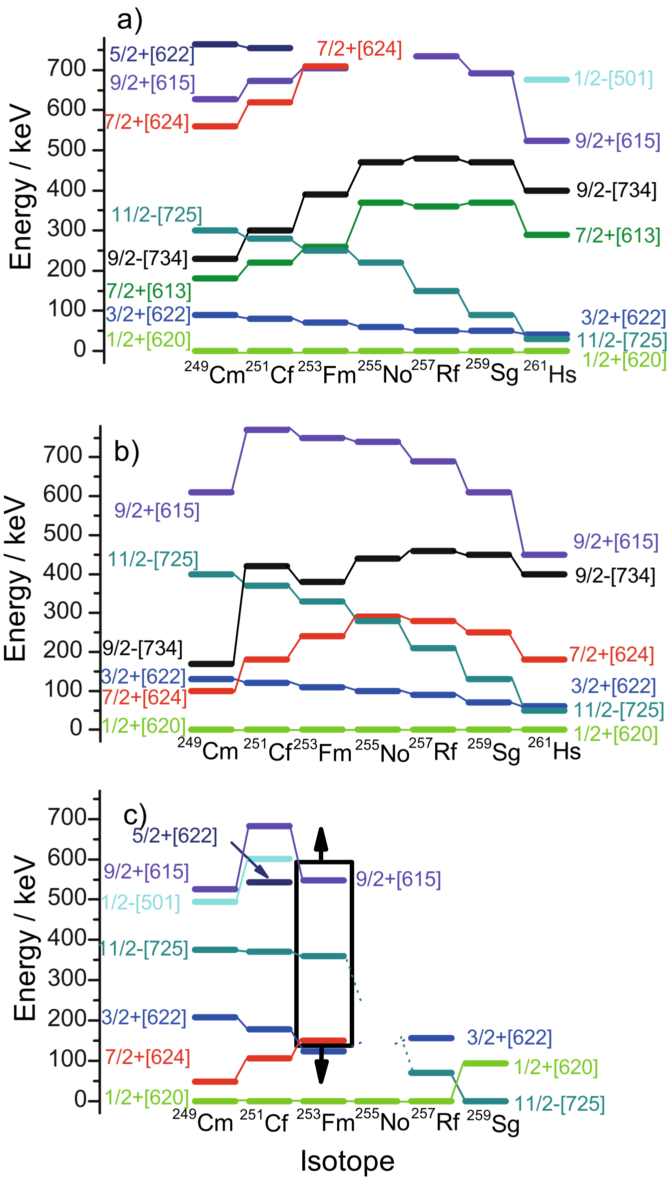

Fig. 9. (Colour on-line) Single-particle level systematics of $N = 153$ isotones. In the upper panels (a) and (b) calculated single-particle states according to different models are displayed. Panel (a) by A. Parkhomenko and A. Sobiczewski [4] and by S. Ćwiok *et al.* [2]. In panel (c) experimental results are shown. Previously known data are taken from ENSDF [27]. Data for ^{253}Fm were obtained in previous studies at SHIP [41]. Values for ^{259}Sg are from this paper.

7.3 Systematics for N = 153 and N = 151 isotones

In recent years several papers with new results related to the systematics of single-particle states in isotones with 153 neutrons were published, the works aimed at the study of ^{255}No [9,11] and ^{257}Rf [13]. They confirmed the ground-state assignment for both isotopes as $1/2^+[620]$ which is predicted as the ground state for all isotones at least up to the ^{261}Hs (see fig. 9 panels (b) and (c)) [2,4].

The $11/2^-[725]$ Nilsson level is known as an isomeric state in several lighter $N = 153$ isotones — in ^{249}Cm at an excitation energy, $E_{exc} = 375$ keV with a half-life of (19 ± 1) ns [39], in ^{251}Cf at $E_{exc} = 370.4$ keV with $T_{1/2} = (1.3 \pm 0.1)$ μs [40] and in ^{253}Fm at $E_{exc} \approx (340–360)$ keV and $T_{1/2} = (0.56 \pm 0.06)$ μs [41]. This state was also assigned to the long-lived isomeric state with $T_{1/2} = (4.9 \pm 0.7)$ s in ^{257}Rf located at $E_{exc} \approx 70$ keV [13]. The regular trend of decreasing excitation energies for $11/2^-[725]$ level is qualitatively in line with theoretical calculations [2,4]. However the significantly lower excitation energy, indicates a faster decrease of its energy than is expected by theory. Therefore one could expect the possibility that the 11/2$^-$[725] state could become the ground state of ^{259}Sg as the next member of the $N = 153$ isotones.

Our results for ^{259}Sg, discussed in this paper, indeed prove this idea and for the first time show the exchange of both levels. The 11/2$^-$[725] state becomes the ground state, while the 1/2$^+$[620] is an excited isomeric state. In previous studies of nuclei in this region a correlation between the energy difference of single-particle levels and predicted β_2 deformation was demonstrated (see, *e.g.*, excitation energy for 7/2$^-$[514] level in odd-mass isotopes of einsteinium [5, 6]). However, calculated single-particle energies presented in a recent study on ^{251}Fm [11] did not show a significant dependence of the energy difference between 1/2$^+$[620] and 11/2$^-$[725] states with any of deformation parameters $\beta_{2,4,6}$.

The results obtained for ^{255}Rf allow to extend the single-particle level systematics for isotones with 151 neutrons. Figures 10(a) and (b) show theoretical predictions [2, 4]. The ground-state assignment on the basis of experimental data (see fig. 10(c)) agrees with the theoretical predictions. However, experimental data already from previous studies [9–13] indicated an interchange in the ordering of the first two excited levels compared to the theoretical predictions (see fig. 10). This replacement of 5/2$^+$[622] and 7/2$^+$[624] states leads to the existence of isomeric states, typically at (140–250) keV with (15–50) μs half-life. In ^{255}Rf the 5/2$^+$[622] state is located at ≈ 135 keV with (50 ± 17) μs half-life.

8 Summary

We presented new data on detailed decay spectroscopy of ^{259}Sg and excited levels in ^{255}Rf. The results allow to extend and improve single-particle level systematics for $N = 151$ and $N = 153$ isotones. We observed a new isomeric state in ^{259}Sg which exists due to the close lying levels 11/2$^-$[725] and 1/2$^+$[620]. The excitation energy for 11/2$^-$[725] exhibits steep decrease and we observed for the first time the change of the ground-state configuration in $N = 153$ isotones from 1/2$^+$[620] to 11/2$^-$[725] at $Z = 106$, expected by theory for heavier elements.

We observed also a new isomeric state in ^{255}Rf caused by the presence of the 5/2$^+$[622] state as the lowest Nilsson level above the ground state. This result extends the known systematics of these isomers in $N = 151$ isotones located typically at (140–250) keV.

Although the energy differences between the predicted theoretical values and experimental data for single-particle levels in the discussed isotopes are rather small, usually up to the several 100 keV, a different ordering of low-lying single-particle levels is evident for several cases. Such re-ordering may completely change the expected decay properties of the nucleus. For example, according to the presented theoretical calculations the 5/2$^+$[622] isomers with half-lives of $\approx$ (15–50) μs should not exist and the ground states of ^{259}Sg and ^{255}Rf should be connected only by very weak α-decay transition because of their large spin difference and different parities. This example shows how critical the information on the single-particle level structure is for describing the decay properties of nuclei in the trans-fermium region.

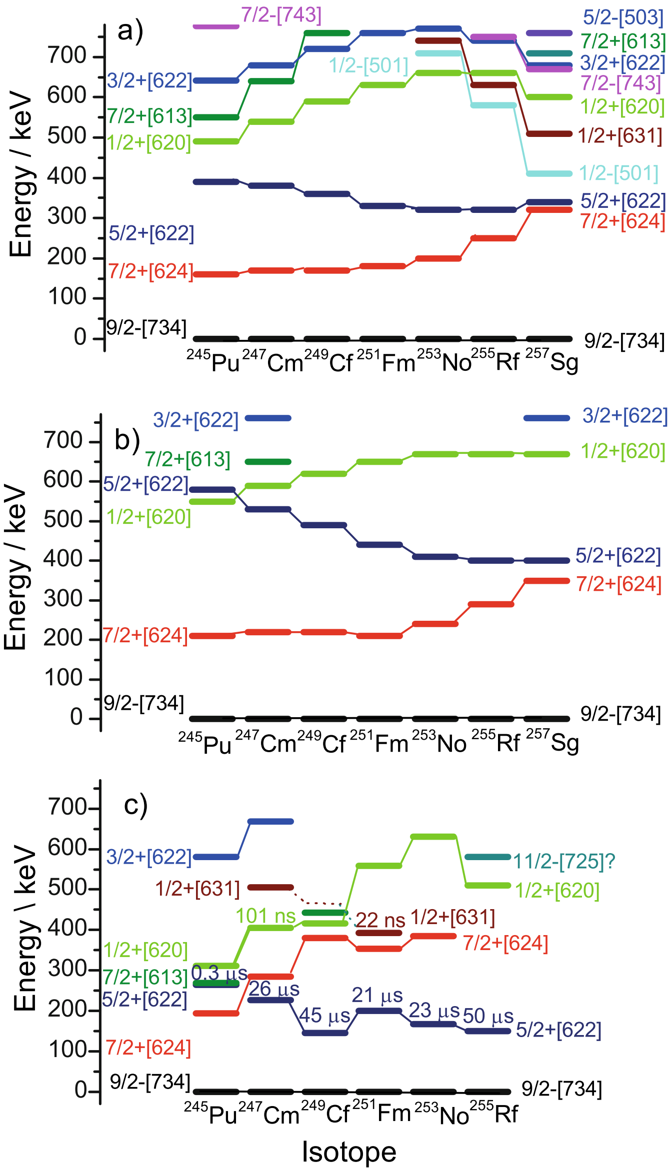

Fig. 10. (Colour on-line) Single-particle level systematics of $N = 151$ isotones. In the upper panels (a) and (b) calculated single-particle states according to different models are displayed. Panel (a) by A. Parkhomenko and A. Sobiczewski [4] and by S. Ćwiok *et al.* [2]. In panel (c) experimental results are shown. Previously known data are taken from ENSDF [27]. Values for excited levels in ^{255}Rf are from this work. The half-life for the single-particle isomer in ^{253}No is taken from our previous studies [41]. The ground-state assignment of ^{255}Rf was done already in previous work [26].

We presented also the fission data for ^{259}Sg and ^{255}Rf, specifically total kinetic energies and fission branching ratios. The evaluated TKE values are $E_{TKE,^{255}\mathrm{Rf}} = (199 \pm 3)$ MeV for ^{255}Rf and $E_{TKE,^{259}\mathrm{Sg}} = (209 \pm 11)$ MeV for ^{259}Sg.

We want to express our gratitude to H.G. Burkhard and J. Maurer for skillful maintenance of the mechanical and electrical components of SHIP. We thank the UNILAC staff for delivering beams of high and stable intensity. This work has been supported by the European Community FP7 - Capacities, contract ENSAR n° 262010, by the Slovak Research and Development Agency (contract No. APVV-0105-10) and by Slovak grant agency VEGA (contract No. 1/0576/13). Financial support by Helmholtz Institute Mainz is acknowledged.

References

1. R.D. Herzberg, P.T. Greenlees, Prog. Part. Nucl. Phys. **61**, 674 (2008).
2. S. Ćwiok, S. Hofmann, W. Nazarewicz, Nucl. Phys. A **573**, 356 (1994).
3. A. Parkhomenko, A. Sobiczewski, Acta Phys. Pol. B **35**, 2447 (2004).
4. A. Parkhomenko, A. Sobiczewski, Acta Phys. Pol. B **36**, 3115 (2005).
5. F.P. Heßberger, S. Antalic, B. Streicher, S. Hofmann, D. Ackermann, B. Kindler, I. Kojouharov, P. Kuusiniemi, M. Leino, B. Lommel *et al.*, Eur. Phys. J. A **26**, 233 (2005).
6. A. Chatillon, Ch. Theisen, P.T. Greenlees, G. Auger, J.E. Bastin, E. Bouchez, B. Bouriquet, J.M. Casandjian, R. Cee, E. Clément *et al.*, Eur. Phys. J. A **30**, 397 (2006).
7. F.P. Heßberger, S. Hofmann, D. Ackermann, P. Cagarda, R.-D. Herzberg, I. Kojouharov, P. Kuusiniemi, M. Leino, R. Mann, Eur. Phys. J. A **22**, 417 (2004).
8. A. Lopez-Martens, K. Hauschild, A.V. Yeremin, A.V. Belozerov, Ch. Briançon, M.L. Chelnokov, V.I. Chepigin, D. Curien, O. Dorvaux, B. Gall *et al.*, Phys. Rev. C **74**, 044303 (2006).
9. F.P. Heßberger, S. Hofmann, D. Ackermann, S. Antalic, B. Kindler, I. Kojouharov, P. Kuusiniemi, M. Leino, B. Lommel, R. Mann *et al.*, Eur. Phys. J. A **29**, 165 (2006).
10. A. Lopez-Martens, K. Hauschild, A.V. Yeremin, O. Dorvaux, A.V. Belozerov, Ch. Briançon, M.L. Chelnokov, V.I. Chepigin, D. Curien, P. Désesquelles *et al.*, Eur. Phys. J. A **32**, 245 (2007).
11. M. Asai, K. Tsukada, H. Haba, Y. Ishii, T. Ichikawa, A. Toyoshima, T. Ishii, Y. Nagame, I. Nishinaka, Y. Kojima, K. Sueki, Phys. Rev. C **83**, 014315 (2011).
12. J. Qian, A. Heinz, T.L. Khoo, R.V.F. Janssens, D. Peterson, D. Seweryniak, I. Ahmad, M. Asai, B.B. Back, M.P. Carpenter *et al.*, Phys. Rev. C **79**, 064319 (2009).
13. B. Streicher, F.P. Heßberger, S. Antalic, S. Hofmann, D. Ackermann, S. Heinz, B. Kindler, J. Khuyagbaatar, I. Kojouharov, P. Kuusiniemi *et al.*, Eur. Phys. J. A **45**, 275 (2010).
14. G. Münzenberg, W. Faust, S. Hofmann, P. Armbruster, Nucl. Instrum. Methods **161**, 65 (1979).
15. S. Hofmann, G. Münzenberg, Rev. Mod. Phys. **72**, 733 (2000).
16. S. Hofmann, W. Faust, G. Münzenberg, W. Reisdorf, P. Armbruster, K. Güttner, H. Ewald, Z. Phys. A **291**, 53 (1979).
17. S. Hofmann, G. Münzenberg, W. Faust, T. Kitahara, W. Reisdorf, P. Armbruste, K. Güttner, B. Thuma, *GSI Jahresbericht 1978* (1979) GSI 79-11, 65.
18. G.D. Jones, Nucl. Intrum. Methods A **488**, 471 (2002).
19. Š. Šáro, R. Janík, S. Hofmann, H. Folger, F.P. Heßberger, V. Ninov, H.J. Schött, A.P. Kabachenko, A.G. Popeko, A.V. Yeremin, Nucl. Instrum. Methods A **381**, 520 (1996).
20. S. Hofmann, D. Ackermann, S. Antalic, H.G. Burkhard, V.F. Comas, R. Dressler, Z. Gan, S. Heinz, J.A. Heredia, F.P. Heßberger *et al.*, Eur. Phys. J. A **32**, 251 (2007).
21. F.P. Heßberger, S. Hofmann, B. Streicher, B. Sulignano, S. Antalic. D. Ackermann, S. Heinz, B. Kindler, I. Kojouharov, P. Kuusiniemi *et al.*, Eur. Phys. J. A **41**, 145 (2009).
22. J.F. Ziegler, J.P. Biersack, SRIM-2013, *Stopping and Range of Ions in Matter*, `www.srim.org`.
23. D.N. Poenaru, M. Ivascu, D. Mazilu, J. Phys. Lett. **41**, L-589 (1980).
24. E. Rurarz, Acta Phys. Pol. B **14**, 917 (1983).
25. C.M. Folden III, I. Dragojević, Ch.E. Düllmann, R. Eichler, M.A. Garcia, J.M. Gates, S.L. Nelson, R. Sudowe, K.E. Gregorich, D.C. Hofmann *et al.*, Phys. Rev. C **79**, 027602 (2009).
26. F.P. Heßberger, S. Hofmann, D. Ackermann, S. Antalic, B. Kindler, I. Kojouharov, P. Kuusiniemi, M. Leino, B. Lommel, R. Mann *et al.*, Eur. Phus. J. A **30**, 561 (2006).
27. *Evaluated Nuclear Structure Data File (ENSDF)*, `http://www.nndc.bnl.gov/`.
28. K.-H. Schmidt, C.-C. Sahm, K. Pielenz, H.-G. Clerc, Z. Phys. A **316**, 19 (1984).
29. Z.G. Gan, Z. Qin, H.M. Fan, X.G. Lei, Y.B. Xu, J.J. He, H.Y. Liu, X.L. Wu, J.S Guo, X.H. Zhou *et al.*, Eur. Phys. J. A **10**, 275 (2001).
30. S. Antalic, F.P. Heßberger, S. Hofmann, D. Ackermann, S. Heinz, B. Kindler, I. Kojouharov, P. Kuusiniemi, M. Leino, B. Lommel *et al.*, Eur. Phys. J. A **38**, 219 (2008).
31. D. Kaji, K. Morimoto, N. Sato, T. Ichikawa, E. Ideguchi, K. Ozeki, H. Haba, H. Koura, Y. Kudou, A. Ozawa *et al.*, J. Phys. Soc. Jpn. **78**, 035003 (2009).
32. I. Dragojevic, K.E. Gregorich, Ch.E. Dullmann, J. Dvorak, P.A. Ellison, J.M. Gates, S.L. Nelson, L. Stavsetra, H. Nitsche, Phys. Rev. C **79**, 011602 (2009).
33. F.P. Heßberger, S. Hofmann, D. Ackermann, V. Ninov, M. Leino, G. Münzenberg, S. Saro, A. Lavrentev, A.G. Popeko, A.V. Yeremin, Ch. Stodel, Eur. Phys. J. A **12**, 57 (2001).
34. K. Nishio, S. Hofmann, F.P. Heßberger, D. Ackerman, S. Antalic, V.F. Comas, Z. Gan, S. Heinz, J.A. Heredia, H. Ikezoe *et al.*, AIP Conf. Proc. **891**, 71 (2007).
35. V.E. Viola, K. Kwiatkowski, M. Walker, Phys. Rev. C **31**, 1550 (1985).
36. F.P. Heßberger, S. Hofmann, V. Ninov, P. Armbruster, H. Folger, G. Münzenberg, H.J. Schött, A.G. Popeko, A.V. Yeremin, A.N. Andreyev, S. Saro, Z. Phys. A **359**, 415 (1997).
37. J. Randrup *et al.*, Nucl. Phys. A **217**, 221 (1973).
38. D.C. Hoffman *et al.*, Nucl. Phys. A **502**, 21c (1989).
39. T. Ishii, H. Makii, M. Asai, K. Tsukada, A. Toyoshima, M. Matsuda, A. Makishima, S. Shigematsu, J. Kaneko, T Shizuma *et al.*, Phys. Rev. C **78**, 054309 (2008).
40. I. Ahmad, F.T. Porter, M.S. Freedman, R.F. Barnes, R.K. Sjoblom, F. Wagner, Jr., J. Milsted, P.R. Fields, Phys. Rev. C **3**, 390 (1971).
41. S. Antalic, F.P. Heßberger, D. Ackermann, S. Heinz, S. Hofmann, Z. Kalaninová, B. Kindler, J. Khuyagbaatar, I. Kojouharov, P. Kuusiniemi *et al.*, Eur. Phys. J. A **47**, 62 (2011).